Available online at www.sciencedirect.com
ScienceDirect
Trans. Nonferrous Met. Soc. China 23(2013) 1019−1027
Transactions of Nonferrous Metals Society of China
www.tnmsc.cn

Photocatalytic activity and kinetics for acid yellow degradation over surface composites of TiO_2-coated activated carbon under different photocatalytic conditions

Meng-xiong ZENG, You-ji LI, Ming-yuan MA, Wei CHEN, Lei-yong LI

College of Chemistry and Chemical Engineering, Jishou University, Jishou 416000, China

Received 3 March 2012; accepted 11 July 2012

Abstract: TiO_2-coated activated carbon surface (TAs) composites were prepared by a sol−gel method with supercritical pretreatment. The photocatalytic degradation of acid yellow (AY) was investigated under UV radiation to estimate activity of catalysts and determine the kinetics. And the effects of parameters including the initial concentration of AY, light intensity and TiO_2 content in catalysts were examined. The results indicate that TAs has a higher efficiency in decomposition of AY than P25, pure TiO_2 particles as well as the mixture of TiO_2 powder and active carbon. The photocatalytic degradation rate is found to follow the pseudo-first order kinetics with respect to the AY concentration. The new kinetic model fairly resembles the classic Langmuir-Hinshelwood equation, and the rate constant is proportional to the square root of the light intensity in a wide range. However, its absorption performance depends on the surface areas of catalysts. The model fits quite well with the experimental data and elucidates phenomena about the effects of the TiO_2 content in TAs on the degradation rate.

Key words: photocatalysis; TiO_2-coated activated carbon; acid yellow; composite catalyst

1 Introduction

In recent years, there has been great interest in the use of advanced oxidation processes (AOPs) for the destruction of hazardous and refractory organic compounds, due to the high oxidation potential of active oxygen species such as OH· and O_2^-· which are generated from irradiated semiconductor catalyst particles [1−5]. Among the AOPs, the photocatalytic oxidation of toxic organic compounds over TiO_2 semiconductor is an emerging technology. TiO_2 photocatalyst has attracted great interest in environmental clean-up operations due to its non-toxic nature, photochemical stability and low cost [6,7]. However, the shortcomings of conventional powder catalysts lie in the low efficiency in making use of light irradiation, and the difficulty in separation after photocatalysis [8]. These disadvantages of TiO_2 catalysts result in a low efficiency of the photocatalytic activity in practical applications. To achieve rapid and efficient decomposition of organic pollutants and easy manipulation, it may be effective to load photocatalysts onto suitably fine adsorbents to concentrate the pollutants around the photocatalysts. Therefore, recent works focused on the preparation, as well as modification of TiO_2 and some composites like SiO_2/TiO_2, ZrO_2/TiO_2 and TiO_2-coated polystyrene spheres were proposed [9−12]. Surprisingly, TiO_2-coated carbon showed high activity in the decomposition of polyvinyl alcohol in water under UV irradiation and was able to be used repeatedly [13]. MATOS et al investigated the influence of different activated carbons on the photocatalytic degradation of aqueous organic pollutants by UV-irradiated titania [14]. TiO_2-coated exfoliated graphite could pump up heavy oils into macropores of exfoliated graphite, where heavy oil pumped was decomposed by TiO_2 under UV irradiation [15]. Large surface area and high degree of dispersion of TiO_2 powders in the reaction media were reported to be favorable for high photocatalytic performance. However, the conventional preparation technologies usually suffer from their inherent disadvantages in the synthesis of TiO_2/activated carbon. For example, deposition of TiO_2 nanoparticles in pores and agglomeration between neighboring TiO_2 particles on pore mouth of porous

Foundation item: Project (50802034) supported by the National Natural Science Foundation of China; Project (11A093) supported by the Key Project Foundation by the Education Department of Hunan Province, China
Corresponding author: You-ji LI; Tel: +86-13762157748; E-mail: bcclyj@163.com
DOI: 10.1016/S1003-6326(13)62561-3

support often cause great decrease in surface area of composites, which weakens the effect of increase of composite surface area. Additionally, since the photocatalytic reaction is light-excited, TiO_2 on the external surface will have more chances to receive light. Therefore, the development of the deposition technique that can maintain high surface area and excellent physicochemical properties of TiO_2 for photocatalysis is thus required. However, few efforts have been made to prepare photocatalyst coated on porous material surface. On the basis of these studies, we attempted to prepare novel photocatalytic materials such as TiO_2-coated activated carbon surface (TAs) composites.

In addition, composites such as TiO_2/carbon [13−15] have been reported to show a synergistic effect on the efficient degradation of some organic compounds in the photocatalytic process [16]. Although the basic principles of photocatalysis over illuminated TiO_2 are well established, the model of a photocatalytic process can be quite a complicated matter as it introduces light intensity to the classical aspects of heterogeneous catalytic systems [17−20]. The non-first-order kinetic behavior was affected by the initial organic content and could be commonly described in terms of a modified Langmuir-Hinshelwood (L−H) model, which has been successfully used for heterogeneous photocatalytic degradation to determine the relationship between the apparent first-order rate constant and the initial content of the organic substrate as follows [2]:

$$\begin{cases} r = -\dfrac{\mathrm{d}C}{\mathrm{d}t} = \dfrac{k_{\mathrm{r}}K_{\mathrm{S}}C}{1+K_{\mathrm{S}}C_0} = k_{\mathrm{app}}C \\ \dfrac{1}{k_{\mathrm{app}}} = \dfrac{1}{k_{\mathrm{r}}K_{\mathrm{S}}} + \dfrac{C_0}{k_{\mathrm{r}}} \end{cases} \tag{1}$$

where C_0 is the initial organic content, k_{r} is the reaction rate constant and K_{S} is the adsorption rate constant.

It was obviously found that Eq. (1) shows the dependence of reaction rate on initial organic content. However, the rate constant k_{r} in the L−H model is independent of the light intensity, which greatly affects photocatalytic rate. So, the real meanings of the parameters (k_{r}) in the L–H model have not been clarified [19,20]. Thus, kinetics is related to these factors, that is, initial organic content, light intensity and some parameters, related to the adsorption of TAs catalyst, and these factors should be included into the kinetic model.

In this work, the kinetic characteristics of photocatalytic degradation of acid yellow (AY) were firstly investigated at different initial contents, light intensity and catalyst with different TiO_2 contents in TAs, and then a kinetic model was established to gain quantitative insight into the relationship between the degradation rate and the influencing factors. Meanwhile, experimental work was conducted to test the new kinetic model and elucidate the photocatalytic process based on the kinetic study results.

2 Experimental

2.1 Composite photocatalyst preparation

Activated carbon was used as support, which was prepared by the vapor activation of coconut shell from Henan Province (average particle size of 0.18 cm, surface area of 593 m^2/g, total pore volume of 0.54 cm^3/g). Butyl alcohol (15 mL) used as a plugging agent was dissolved in supercritical CO_2, and then impregnated into the activated carbon (30 g) under the desired supercritical condition to form sealed substrates. The particular preparation by an improved sol−gel method is as follows. Tetrabutyl titanate (10 mL) and diethanolamine (3 mL) were dissolved in ethanol (82 mL). The solution was stirred vigorously at 20 °C, followed by the addition of a mixture of doubly-distilled water and HCl containing ethanol. The resulting alkoxide solution was left at 20 °C for 4 h to hydrolyze to a TiO_2 sol. The desired amount of sealed substrates was immersed into the TiO_2 sol with a certain viscosity, and the mixture was stirred in an ultrasonic bath. When the TiO_2 sol coating on the sealed substrates changed to a TiO_2 gel with ultrasonic treatment, the TiO_2 gel-coated sealing substrates were vacuum dried and subsequently the process from immersing to dryness was repeated. Finally, the particles obtained were first heat-treated at 250 °C for 3 h in air and then at 400 °C in nitrogen for 2 h, which resulted in the prepared TiO_2-coated activated carbon surface (TAs) composites.

The dye under consideration was AY, which is a highly water soluble and widely used as a colorant in textiles, and is also a well-known acid-base record indicator. So, the photodegradation of AY is important with regard to the purification of dye effluents.

2.2 Photocatalytic experimental system

All experiments were carried out in a batch photoreactor shown in Fig. 1. A pyrex reactor cell of 28 cm in height and effective volume of 280 mL was equipped with some faucets. A ultraviolet lamp was positioned inside a pyrex reactor with a wavelength of 320−400 nm and peak wavelength of 365 nm, respectively. AY solution was added into the reactor cell with internal stirring by air sparging with a flow capacity of 38 mL/s. After solution was aeration mixed for about 60 min in dark condition in order to eliminate the effect of TAs adsorption on the photocatalytic rate, the illumination was turned on to start the photocatalytic reaction. The suspension was sampled from the reactor cell by using a glass syringe at timed intervals during

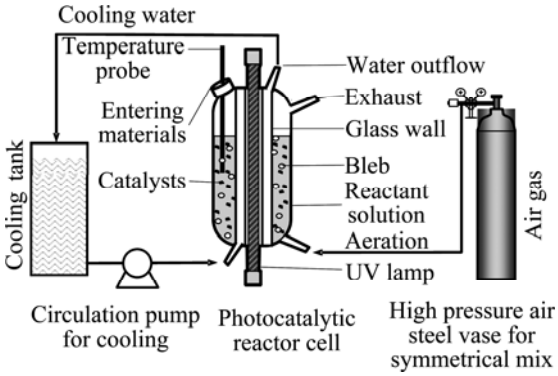

Fig. 1 Experimental system of photocatalytic reaction

degradation and centrifuged immediately for removal of suspended solids. The clean transparent solution was analyzed by UV-Vis spectroscopy (757CRT UV-Vis spectrophotometer, Shanghai) after filtration. The AY content was measured from the absorbance at the wavelength of 358 nm by using a calibration curve. For kinetic analysis purpose, each sample taken from the reactor was divided into three different vials and the final absorption was given by the arithmetic average over three measurements. Repetition tests were made to achieve arithmetic average of the photocatalytic degradation rates.

To probe the dependence of the kinetic characteristics of the photocatalytic degradation upon light intensity, initial organic content and absorption performance of the catalyst (i.e. different TiO_2 content of TAs), a series of experiments were carried out under different photocatalytic conditions. The initial content of AY was varied from 6 to 15 mg/L. The light intensities of UV lamp, applied in the work, were 10, 15, 25 and 40 mW/cm^2, respectively. The aerating rate of air and reacting temperature were controlled at 38 mL/s and 25 °C, respectively. For each group of experiments at certain light intensity, five different AY contents were applied.

2.3 Characterization techniques

The crystalline phase was determined using X-ray diffraction (XRD) (Diffractometer HZG-4, Zeiss, Germany). Samples were also characterized by measuring Brunauer-Emmett-Teller (BET) surface areas by the nitrogen sorption method (ASAP2010, Micromeritics Company, USA) at 77 K. The average pore size was obtained using adsorption data by the Barrett-Joyner-Halenda (BJH) method. The surface morphologies of the raw actived carbon and supported catalysts were also determined by scanning electron microscopy on a SEM Philips S3400-N instrument operating at 25 kV. The AC was completely removed in air flow, and the AC support with TiO_2 was firstly calcined at 250 °C in air for 2 h in order to volatilize and combust organic compounds, and heat-treated for 2 h under the N_2 flow. Therefore, the TiO_2-coating content, $w(TiO_2)$, of the sample calcined under the N_2 flow was determined by

$$w(\mathrm{TiO_2}) = \frac{m(\mathrm{TiO_2})}{m(\mathrm{AC})} = \frac{m(\mathrm{TiO_2})}{m(\mathrm{TAs}) - m(\mathrm{TiO_2})}$$

$$= \frac{m_{900\,^\circ\mathrm{C}}^{\mathrm{Air}}}{m_{900\,^\circ\mathrm{C}}^{\mathrm{N_2}} - m_{900\,^\circ\mathrm{C}}^{\mathrm{Air}}} \quad (2)$$

where $m_{900\,^\circ\mathrm{C}}^{\mathrm{Air}}$ and $m_{900^\circ\mathrm{C}}^{\mathrm{N_2}}$ are the measured masses at 900 °C under the air flow and under the N_2 flow, respectively.

3 Results and discussion

3.1 BET surface and adsorbing performance

AY was adsorbed on the catalyst surface without UV irradiation (in the dark). Adsorption equilibrium for AY was established within 60 min and the adsorbed amount of AY on the catalyst (adsorption capacity, in mass fraction in %) was determined from the measurement of AY concentration before and after adsorption. As shown in Fig. 2, surface area of the composite catalysts decreases with increasing TiO_2 content. The decrease in surface area is evidently non-linear to the TiO_2 content, indicating that the TiO_2 nanoparticles are dispersed inside the AC and cause partial blockage of the pores. BET surface areas of bare TiO_2 (80 m^2/g) prepared by the sol–gel method and Degussa-P25 (48 m^2/g) [21] are much fewer than the present composite catalysts. It is attributed to the coating of the surface of activated carbon with nano-TiO_2 particles. Additionally, the dark adsorption experiments

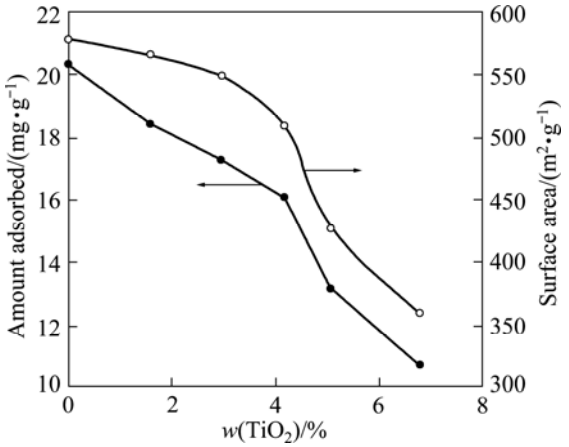

Fig. 2 BET surface area and amount adsorbed AY vs TiO_2 content in TAs

on all the catalysts and original AC show that adsorption decreases only with the increasing content of TiO_2 due to the decreasing surface area of TAs.

X-ray powder diffraction method was used to assess the crystallinity of the catalyst particles. XRD peaks, characteristic of anatase were observed at 2θ=25.38° for TAs (Fig. 3). Peaks corresponding to anatase also appear at 2θ=37.8°, 48.3°, 54.88°. However, no significant peak of rutile is observed at 2θ=27.428°. As expected, with increasing content of TiO_2, sharper peaks of TiO_2 are observed due to the increased crystalline feature of TiO_2. However, low intensity and broad peak characteristic of XRD pattern of TAs compared with that of bare TiO_2 indicate that highly dispersed fine particles of anatase are formed on these supports.

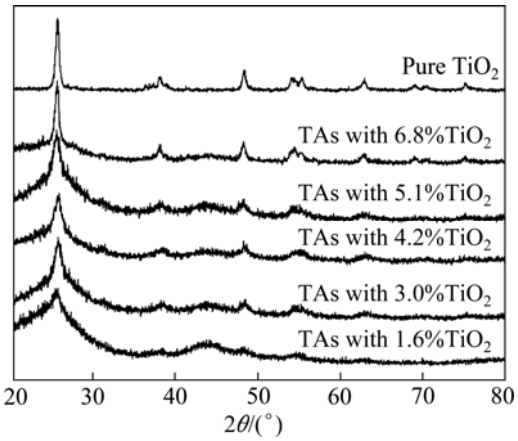

Fig. 3 XRD pattern of pure TiO_2 and TAs with different TiO_2 contents

Morphology of TAs was investigated by SEM. As shown in Fig. 4, The TAs illustrates a kind of uniform morphology with some pores (Fig. 4(a)). Under a larger magnification, the surface of TAs is obviously coated TiO_2 layer with some mesopores in substrate (Fig. 4(b)). It is mainly due to TiO_2 sol coated on surface of sealing substrates and then transited TiO_2 layer in calcination process. It is the main reason that TAs composites retain high surface areas.

3.2 Degradation of acid yellow

Prior to the evaluation of photocatalytic activity of prepared catalysts, the concentration of AY in the aqueous solution decreased before lighting because of adsorption in the dark. Most of the concentration decrease occurred during irradiation. Therefore, the decrease in AY concentration during irradiation was due to the chemical reaction rather than adsorption. For convenience, we assumed that the concentration of AY after desorption–adsorption equilibrium was the initial concentration, ρ_0. Figure 5 shows the degradation

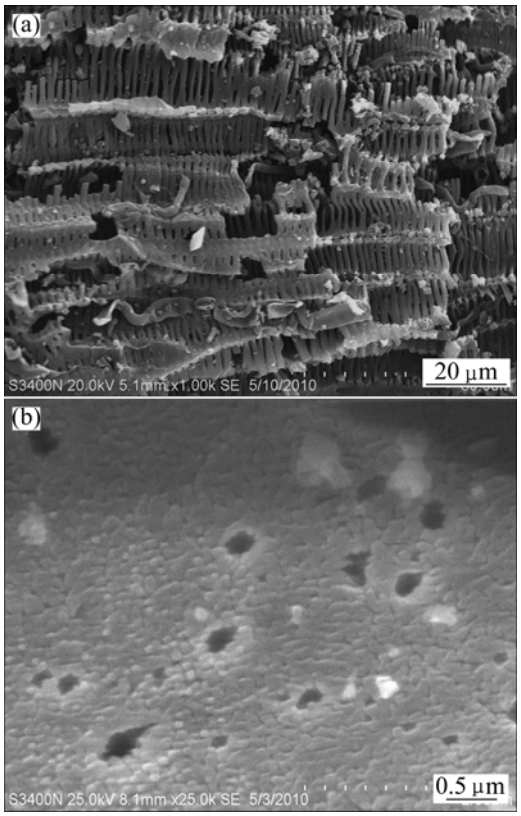

Fig. 4 SEM image of TAs

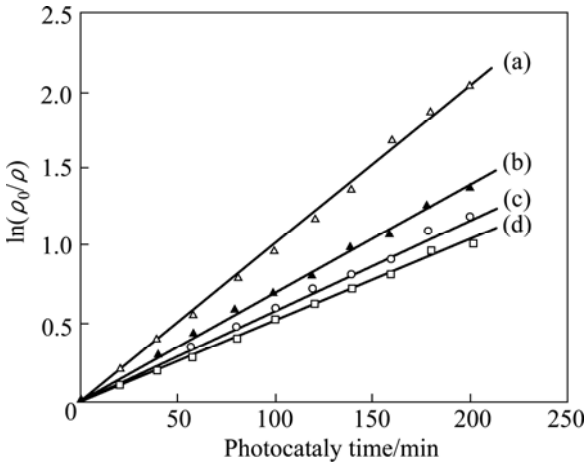

Fig. 5 Photocatalytic degradation of acid yellow by TAs with 6.8%TiO_2 (a), mixture of TiO_2 powder and AC with 6.8% TiO_2 (b), P25 (c) and TiO_2 powder (d) (ρ_0=13 mg/L, I=25 mW/cm^2, [TAs]=3.0 g/L)

of AY as a function of reaction time in the presence of different catalysts. It is found that photodecoloration of AY fits the pseudo-first-order reaction equation. The rate constants k_{app} of AY degradation are found to be 0.0049 and 0.0057 min^{-1} for pure TiO_2 and P25, respectively, while k_{app} for the mixture of TiO_2 and active carbon was 0.0070 min^{-1} and 0.0098 min^{-1} for TAs, respectively. It is found that TAs has the highest photocatalytic activity due to AC as adsorbent for the composite catalysts. The high

surface area of active carbon is effective to concentrate AY around the loaded TiO_2 and produce high concentrations of organic compounds for TiO_2 photocatalyst.

3.3 Effects of initial content of AY, light intensity and TiO_2 content in catalyst on photocatalytic rate

Experiments on the photocatalytic oxidation of AY were conducted in solutions with various AY concentrations: 6, 7.5, 10, 13 and 15 mg/L. The degradation curves of the AY dyestuff induced by the TAs catalyst are well fitted by a mono-exponential curve, suggesting that the degradation experiments under UV irradiation of AY aqueous solutions containing TAs follow the first-order reaction. According to Eq. (1), a plots of $\ln(\rho_0/\rho)$ versus t for all the experiments with different TiO_2 contents in TAs are shown in Fig. 6. The values of apparent rate constant k_{app} can be obtained directly from the slope of regressed linear curve. Figure 6 shows the dependence of k_{app} on the TiO_2 content of TAs, which suggests that the apparent rate constant does not increase monotonously with increasing content of TiO_2. The relation between the AY degradation rate follows the order of TiO_2 content from high to low: 4.2%, 5.1%, 3.0%, 6.8%, 1.6 %.

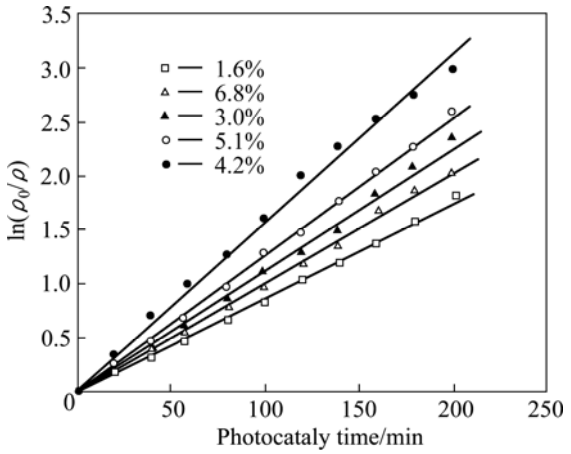

Fig. 6 Effect of TiO_2 content of TAs photocatalysts on photocatalytic degradation of AY (ρ_0=10 mg/L, I=25 mW/cm^2, [TAs]=3.0 g/L)

Additionally, the effects of initial content of AY and light intensity on photocatalytic rate are shown in Fig. 7. The reactant in solution absorbed UV light, which lowed its intensity, resulted in a decrease of the photoactivity of the catalyst. So, the initial concentration of the dyestuff has a negative fundamental effect on the degradation rate, namely, the kinetic rate constant decreases with increasing concentration [22]. It is obvious from the results in Fig. 7 that the apparent rate constant decreases with increasing AY concentration. This could be explained by the following causes: for a certain TAs, the amount of active centers on the photocatalyst is finite, and the molecules of AY are excessive in comparison with the amount of active centers on the photocatalyst, thereby reducing the UV light adsorption capability of the catalyst. Meanwhile, light intensity is a major factor in photocatalytic reactions because electron-hole pairs are produced by light energy [19]. Figure 7 also shows an increase in the degradation rate constant k_{app} of AY with the increasing light intensity for a certain initial organic content. For example, the decomposition rate at 40 mW/cm^2 is faster than that at 25, 15 or 10 mW/cm^2. This is because higher light intensity provides higher energy for more TiO_2 in TAs to produce electron-hole pairs. Besides, it is evidently observed that k_{app} increases by increasing light intensity and decreasing organic content, respectively. Therefore, it is reasonably deduced that the effect of organic content on k_{app} is ascribed to the absorbing light performance of the reactant solution.

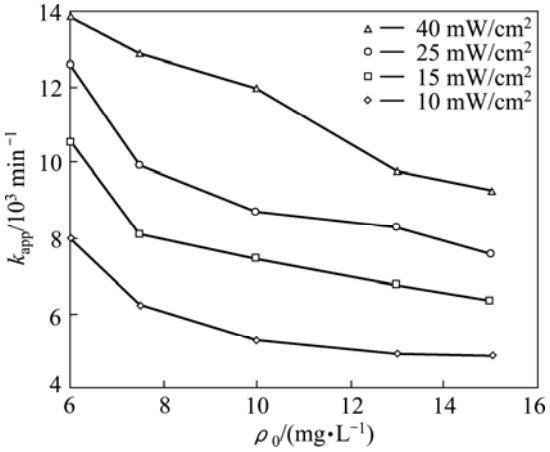

Fig. 7 Effects of initial concentration of AY and light intensity on rate constant k_{app} of AY photodegradation ([TAs]=3.0 g/L; $w(TiO_2)$=1.6%)

3.4 Kinetics model of photocatalytic degradation

Under the experimental conditions, it can be assumed that the first step in reaction is the adsorption of AY molecules and their degradation products on the surface of TAs photocatalyst, and the second step is all adsorbed substrates to be decomposed. Considering this, the assumptions are as follows.

1) Photocatalytic oxidation is mainly completed via the hydroxyl groups absorbed on the surface of the TAs catalyst, which attacks the organic compounds and related intermediates on the catalyst surface. It is the rate-limiting step for photocatalytic degradation.

2) The combination of H_2O/OH^- with the photo-induced holes h^+ to form hydroxyl groups, and the HO· radicals should be mainly formed from the adsorbed H_2O molecules.

3) The combination rate of h^+/e is much more than the hydroxyl forming rate of the reaction among h^+,

H_2O and OH^-.

4) The concentration of hydroxyl radicals is constant at a steady state (Bodenstein steady state assumption).

5) The concentration of h^+ is constant at a steady state (Bodenstein steady state assumption).

6) The deactivation of ·OH radicals with inactive surfaces (S) is more important than other processes. Acknowledging the four reaction steps for photocatalysis, the elementary reaction equations are expressed as

$$h\gamma \xrightarrow{k_1} h^+ + e \xrightarrow{k_2} \text{Heat} \quad (3)$$

$$h^+ + OH^- \xrightarrow{k_3} \cdot OH \quad (4)$$

$$h^+ + H_2O \xrightarrow{k_4} \cdot OH + H^+ \quad (5)$$

$$\cdot OH + AY_{ads} \xrightarrow{k_5} \text{Intermediate} \quad (6)$$

$$\cdot OH + \text{Intermediate} \xrightarrow{k_6} \text{Product} \quad (7)$$

$$\cdot OH + S_{inactive} \xrightarrow{k_7} \text{Inactive species} \quad (8)$$

Reaction (3) refers to the photonic activation step and depicts the recombination step, while reactions (4) and (5) represent the formation of the hydroxyl product, and reactions (6) and (7) show the degradation of AY and its various intermediate degradating decomposition of the product, respectively. According to assumption 1, the photocatalytic degradation rate (r) for the surface decomposition of AY on TAs, is represented as

$$r = k_5[\cdot OH]\alpha_{AY_{ads}} \quad (9)$$

where k_5 is the rate constant, and $\alpha_{AY_{ads}}$ is the fractional site coverage by AY dye. Additionally, according to similar equation deduction [23,24], we obtained the following equation:

$$\alpha_{AY_{ads}} = \frac{K_{AY}\rho}{1 + K_{AY}\rho_0} \quad (10)$$

where ρ_0 and K_{AY} are the initial concentration and adsorption rate constants of AY, respectively.

Considering the Bodenstein steady state assumption (assumption 4), the concentration of hydroxyl groups, [·OH], is constant, then,

$$\frac{d[\cdot OH]}{dt} = k_3[h^+][OH^-] + k_4[h^+][H_2O] - k_5[\cdot OH]\alpha_{AY_{ads}} - k_6[\cdot OH][Int.] - k_7[\cdot OH]S_{inactive} \approx 0 \quad (11)$$

According to assumption 6, we can obtain

$$k_3[h^+][OH^-] + k_4[h^+][H_2O] - k_5[\cdot OH]\alpha_{AY_{ads}} - k_6[\cdot OH][Intermediate] - k_7[\cdot OH]S_{inactive} = [h^+](k_3[OH^-] + k_4[H_2O]) - k_7[\cdot OH]S_{inactive} \approx 0 \quad (12)$$

And

$$[\cdot OH] = \frac{k_8[h^+]}{k_7 S_{inactive}} = k'[h^+] \quad (13)$$

where k_8 is equal to sum of $k_3[OH^-]$and $k_4[H_2O]$, meanwhile, k' is equal to $k_8/(k_7S_{inactive})$.

The concentration of photo-induced holes, $[h^+]$, can be obtained by applying assumption 5 to the following equation:

$$\frac{d[h^+]}{dt} = k_1 I - k_2[h^+]^2 - k_3[h^+][OH^-] - k_4[h^+][H_2O] \approx 0 \quad (14)$$

$$\frac{d[h^+]}{dt} = k_1 I - k_2[h^+]^2 - k_8[h^+] \approx 0$$

ROTHENBERGER et al [25] applied laser pulse photolysis to determine the recombination rate coefficient of the separated e and h^+, in which k_2 is much higher than k_3. According to assumption 3, $k_8[h^+] << k_2[h^+]^2$. Consequently, $[h^+]$ has the following form:

$$[h^+] = \left(\frac{k_1 I}{k_2}\right)^{1/2}$$

$$[\cdot OH] = k'[h^+] = k'\left(\frac{k_1 I}{k_2}\right)^{1/2}$$

$$r = k_5[\cdot OH]\alpha_{AY_{ads}} = k_5 k'\left(\frac{k_1 I}{k_2}\right)^{1/2}\frac{K_{AY}\rho}{1 + K_{AY}\rho_0} \quad (15)$$

In the stage, Eq. (15) can be written as

$$r = k''\frac{I^{1/2}K_{AY}\rho}{1 + K_{AY}\rho_0} = k_{app}\rho$$

with

$$k'' = k_5 k'\left(\frac{k_1}{k_2}\right)^{1/2}$$

When light intensity is constant, we can obtain

$$1/k_{app} = 1/(k_r K_{AY}) + \rho_0/k_r \quad (16)$$

$$k_r = k''I^{1/2} \quad (17)$$

3.5 Model fitting to experimental data

Figure 8 shows a plot of $1/k_{app}$ versus ρ_0 for different light intensities. The value of the rate constant, k_r, is obtained by linear regression of the points calculated by Eq. (16). In Eq. (17), the model parameter k_r shows a dependence on the square root of light intensity I, that is, $k_r = k''I^{1/2}$, where k'' is the equation coefficients determined by elementary reactions rather than light intensity. Based on the assumption that the kinetic model is valid, k_r is plotted versus $I^{1/2}$ based on the experimental data, as shown in Fig. 9. k_r is almost well correlated to $I^{1/2}$, which supports the validity of Eq. (17).

Consequently, the parameter k_r in the present study is regressed as follows:

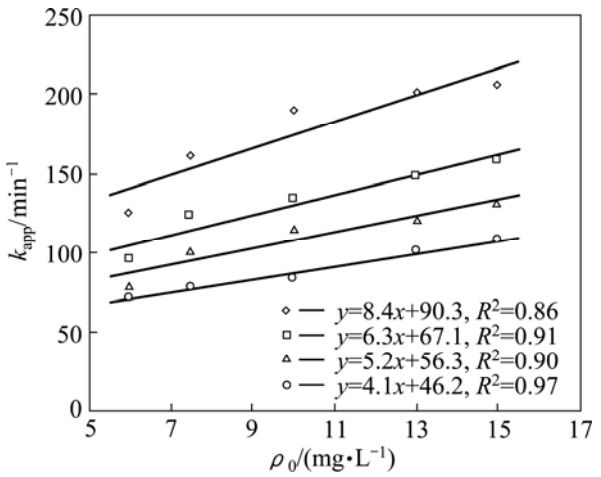

Fig. 8 Relationship between $1/k_{app}$ and ρ_0 with different light intensities (◇—10 mW/cm^2; □—15 mW/cm^2; △—25 mW/cm^2; ○—40 mW/cm, [TAs]=3.0 g/L; $w(TiO_2)$=1.6%)

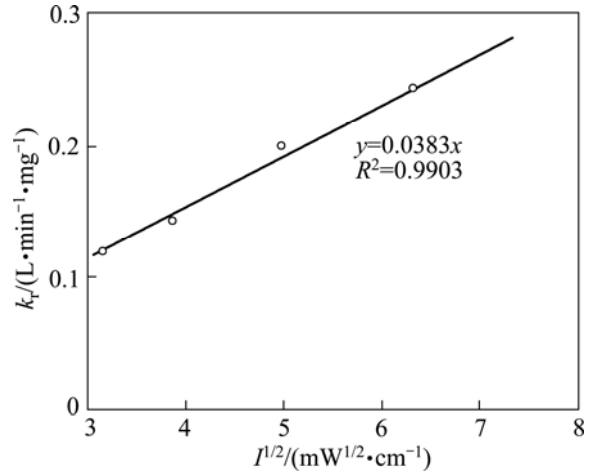

Fig. 9 Dependence of k_r on square root of light intensity

$$k_r=0.0383I^{1/2} \quad (18)$$

Based on the model, k_r is made up of two parts, one constant and the other intensity-dependent. Chiefly, compared with the classic L−H mode, our kinetic model shows that k_r is dependent on a square root of light intensity. Since the correlation coefficient of Eq. (18) is high and reaches 0.9903, the equation for the results in Fig. 9 fits well with the experimental data. Furthermore, we show that some predictions coincide well with the experimental results and indicate the effects of light intensity on the rate constant by using the equations for the present investigation.

3.6 Relationship between TiO_2 content and photoactivity

Under the same experimental conditions, Eq. (16) was obtained for TAs with different TiO_2 contents, as listed in Table 1. The dependence of the rate constant k_r and adsorption performance of TAs was determined based on the TiO_2 content of TAs when the light intensity was invariable. By comparison, at the same light intensity, it is obvious that the rate constant k_r firstly increases with increasing TiO_2 content, but then decreases, and the relation between the rate constant k_r and TiO_2 content in TAs follows the dropping sequence of 4.2%, 5.1%, 6.8%, 3.0%, 1.6%, while the adsorption decreases monotonously with increasing TiO_2 content (Fig. 2). It can be assumed that the AY decomposition rate for the TAs is mostly determined by TiO_2 particles for its catalytic effect. But the surface area of the catalyst is also an important factor affecting the photoactivity of the catalyst. For the catalyst with 1.6% TiO_2, the exceptionally high adsorption performance shows a lower degradation rate presumably due to the low TiO_2 content. After passing a maximum, the rate constant decreases with increasing TiO_2 content, which may be due to the decreasing amount of adsorbed AY, which drastically decreases as a result of the reduced surface area. The rate constant k'' firstly increases with increasing TiO_2 content in TAs, but then decreases, which is consistent with the relation between k_r and the TiO_2 content of TAs. The coefficient values, listed in Table 1 for different TAs, are more than 0.98. This proves that the models fit well with the experimental data and the above assumptions are fairly rational.

Table 1 Rate constant k_r of acid yellow photodegradation with different TiO_2 contents in TAs, and corresponding parameters and correlation coefficient (R^2)

$w(TiO_2)$/%	k_r equation	K''	R^2
1.6	$k_r=0.0383I^{1/2}$	0.0383	0.9903
3.0	$k_r=0.0452I^{1/2}$	0.0452	0.9784
4.2	$k_r=0.0716I^{1/2}$	0.0716	0.9871
5.1	$k_r=0.0696I^{1/2}$	0.0693	0.9863
6.8	$k_r=0.0548I^{1/2}$	0.0548	0.9910

The AY initial content range is from 6 to 15 mg/L with range of light intensity form 10 to 40 mW/cm^2.

4 Conclusions

The kinetic characteristics of the photocatalytic degradation of acid yellow by a TiO_2-coated activated carbons catalyst (TAs) were experimentally investigated with respect to the initial AY content, different light intensities, and different TiO_2 contents in the TAs. The kinetic characteristics were ascertained to follow the first-order model. However, the dependence of the apparent rate constant k_{app} on the light intensity, initial

content of AY and the TiO_2 content in the TAs were observed. To account for the experimental results, a new kinetic model, which fairly resembles the classic Langmuir-Hinshelwood equation from its expression, was proposed on the basis of intrinsic elemental reactions. This correlates light intensity with the parameters in the new model and further predicts that k_r is linear with respect to the square root of the intensity over a wide intensity range, which suggests that the kinetic model is rationally deduced on the basis of some valid assumptions.

References

[1] WANG R M, CHU C L, HU T, DONG Y S, GUO C, SHENG X B, LIN P H, CHUNG C Y, CHU P K. Surface XPS characterization of NiTi shape memory alloy after advanced oxidation processes in UV/H_2O_2 photocatalytic system [J]. Appl Surf Sci, 2007, 253: 8507−8512.

[2] JESUS B D H, JOAQUIN T, JOAQUIN R, DOMINGUEZA J A P. Oxidation of *p*-hydroxybenzoic acid by UV radiation and by TiO_2/UV radiation: Comparison and modelling of reaction kinetic [J]. Hazard Mater, 2001, B83: 255−264.

[3] CHACON J M, LEAL M T, SANCHEZ M, BANDALA E R. Solar photocatalytic degradation of azo-dyes by photo-Fenton process [J]. Dyes Pigments, 2006, 69: 144−150.

[4] LI Ai-chang, LUO Peng-fei, LIU Ying. Hydrogen evolution properties of (Ni−W−P)−TiO_2 composite coating as electrode materials prepared by electrolytic co-deposition [J]. The Chinese Journal of Nonferrous Metals, 2010, 20(4): 712−717. (in Chinese)

[5] AN T, YANG H, LI G Y, SONG W H, COOPER W L J, NIE X P. Kinetics and mechanism of advanced oxidation processes (AOPs) in degradation of ciprofloxacin in water [J]. Appl Catal B Environ, 2010, 94: 288−294.

[6] KHODJA A A, SEHILI T, PILICHOWSKI J F, BOULE P. Photocatalytic degradation of 2-phenylphenol on TiO_2 and ZnO in aqueous suspensions [J]. J Photochem Photobiol A, 2001, 141: 231−239.

[7] CHONG M N, JIN B, CHOW C W K, SAINT C. Recent developments in photocatalytic water treatment technology: A review [J]. Water Res, 2010, 44: 2997−3027.

[8] HOLGADO M, CINTAS A, IBISATE M, SERNA C J, LOPEZ C, MESEGUER F. Three-dimensional arrays formed by monodisperse TiO_2 coated on SiO_2 spheres [J]. J Colloid Interface Sci, 2000, 229: 6−11.

[9] YIN Yan-sheng, GUAN Kai-shu, ZHAO Hong. Effect of SiO_2 addition on surface structural and super-hydrophilic property of TiO_2 films [J]. The Chinese Journal of Nonferrous Metals, 2003, 13(2): 437−441. (in Chinese)

[10] FUKAHORI S, ICHIURA H, KITAOKA T, TANAKA H. Removal of indoor po11utants under UV irradiation by a composite $Ti0_2$-zeolite sheet [J]. Appl Catal B, 2003, 46: 453−462.

[11] WANG Xin, TANG Dian, ZHOU Jing-en. Effect of TiO_2 on microstructure of RuO_2 +SnO_2+TiO_2/Ti anode nanometer coatings [J]. The Chinese Journal of Nonferrous Metals, 2003, 13(3): 708−712. (in Chinese)

[12] TADA H, HATTORI A, TOKIHISA Y. A patterned-TiO_2/SnO_2 bilayer type photocatalyst [J]. J Phys Chem, 2000, 104: 4587−4592.

[13] LIU Y, WANG A, CLAUS R. Layer-by-layer electrostatic self-assembly of nanoscale Fe_3O_4 particles and polyimide precursor on silicon and silica surfaces [J]. J Phys Chem, 1997, 101: 1385−1992.

[14] MATOS J, LAINE J, HERMANN J M. Effect of the type of activated carbons on the hotocatalytic degradation of aqueous organic pollutants by UV-irradiated titania [J]. J Catal, 2001, 200: 10−20.

[15] LEE Y C, YANG J W. Self-assembled flower-like TiO_2 on exfoliated graphite oxide for heavy metal removal [J]. J Ind Eng Chem, 2002, 18: 1178−1185.

[16] TSUMURA T, KOJITANI N, UMEMURA H, TOYODA M, INAGAKI M. Composites between photoactive anatase-type TiO_2 and adsorptive carbon [J]. Appl Surf Sci, 2002, 196: 429−436.

[17] LEE D K, KIM S C, KIM S J, CHUNG I S, KIM S W. Photocatalytic oxidation of microcystin-LR with TiO_2-coated activated carbon [J]. Chem Eng J, 2004, 102: 93−98.

[18] XU Y M, LANGFORD C H. Variation of Langmuir adsorption constant determined for TiO_2-photocatalyzed degradation of acetophenone under different light intensity [J]. J Photochem Photobiol A, 2000, 133: 67–71.

[19] DANESHVAR N, RABBANI M, MODIRSHAHLA N, BEHNAJADY M A. Kinetic modeling of photocatalytic degradation of Acid Red 27 in UV/TiO_2 process [J]. J Photochem Photobiol A, 2004, 168: 39−45.

[20] MONTOYA J F, VELASQUEZ J A, SALVADOR P. The direct–indirect kinetic model in photocatalysis: A reanalysis of phenol and formic acid degradation rate dependence on photon flow and concentration in TiO_2 aqueous dispersions [J]. Appl Catal B, 2009, 88: 50−58.

[21] LI Y J, MA M Y, SUN S G, YAN W B, OUYANG Y Z. Preparation of TiO_2–carbon surface composites with high photoactivity by supercritical pretreatment and sol–gel processing [J]. Appl Sur Sci, 2008, 254: 4154−4158.

[22] BHATTACHARYYA A, KAWI S, RAY M B. Photocatalytic degradation of orange II by TiO_2 catalysts supported on adsorbents [J]. Catal Today, 2004, 98: 431−439.

[23] SILVADA C G, FARIA J L. Photochemical and photo-catalytic degradation of an azo dye in aqueous solution by UV irradiation [J]. J Photochem Photobiol A, 2003, 155: 133−143.

[24] KESSELMAN J M, LEWIS N S. HOFFMANN M R. Photoelectrochemical degradation of 4-chlorocatechol at TiO_2 electrodes, comparison between sorption and photoreactivity [J]. Environ Sci Technol, 1997, 31: 2299−2306.

[25] ROTHENBERGER G, MOSER J, GRATZEL M, SERPNE N, SHARMA D K. Charge carrier trapping and recombination dynamics in small semiconductor particles [J]. J Am Chem Soc, 1985, 107: 8054−8059.

外负载 TiO_2/活性炭在不同条件下降解酸性黄的光催化性能及其动力学

曾孟雄，李佑稷，马明远，陈 伟，李雷勇

吉首大学 化学化工学院，吉首 416000

摘 要：以超临界流体沉积法处理过的活性炭(AC)为载体，采用溶胶−凝胶法制备外负载 TiO_2/AC(TAs)光催化材料。在紫外光照射下，通过对可溶性染料酸性黄(AY)的降解反应，考察外负载 TiO_2/AC 复合体的光催化性能并建立光催化降解动力学，同时探讨酸性黄初始溶液浓度、光强度、催化剂浓度对其光催化降解性能的影响。结果表明，TAs 具有很高的光催化活性，对酸性黄的光催化性能比 TiO_2+AC、TiO_2 和 P25 的高。外负载 TiO_2/AC 对不同初始浓度酸性黄的光催化降解符合一级动力学，这种新的动力学模型符合经典的 Langmuir-Hinshelwood 定律且在较大范围内其降解速率常数与光强度的平方根成正比。然而，其吸附性能取决于光催化剂的比表面积。模型与实验数据较吻合，表明此模型能阐明催化剂 TAs 中 TiO_2 浓度对光催化性能的影响。

关键词：光催化；外负载 TiO_2 活性炭；酸性黄；复合体催化剂

(Edited by Xiang-qun LI)